

Published in final edited form as:

*Mol Cell*. 2012 July 13; 47(1): 122–132. doi:10.1016/j.molcel.2012.04.025.

## A direct HDAC4-MAP kinase crosstalk activates muscle atrophy program

Moon-Chang Choi<sup>1,\*</sup>, Todd J. Cohen<sup>1,\*</sup>, Tomasa Barrientos<sup>1</sup>, Bin Wang<sup>1</sup>, Ming Li<sup>1</sup>, Bryan J. Simmons<sup>1</sup>, Jeong Soo Yang<sup>2</sup>, Gregory A. Cox<sup>3</sup>, Ying-Ming Zhao<sup>2</sup>, and Tso-Pang Yao<sup>1,#</sup>

<sup>1</sup>Department of Pharmacology and Cancer Biology, Duke University, Durham, NC 27710

<sup>2</sup>The Ben May Department for Cancer Research, University of Chicago, Chicago, IL 60637

<sup>3</sup>The Jackson Laboratory, 600 Main Street Bar Harbor, ME 04609

### Summary

Prolonged deficits in neural input activate pathological muscle remodeling leading to atrophy. In denervated muscle, activation of the atrophy program requires HDAC4, a potent repressor of the master muscle transcription factor, MEF2. However, the signaling mechanism that connects HDAC4, a protein deacetylase, to the atrophy machinery remains unknown. Here, we identify the AP1 transcription factor as a critical target of HDAC4 in neurogenic muscle atrophy. In denervated muscle, HDAC4 activates AP1-dependent transcription whereas AP1 inactivation recapitulates HDAC4 deficiency and blunts the muscle atrophy program. We show that HDAC4 activates AP1 independently of its canonical transcriptional repressor activity. Surprisingly, HDAC4 stimulates AP1 activity by activating the MAP kinase cascade. We present evidence that HDAC4 binds and promotes the deacetylation and activation of a key MAP3 kinase, MEKK2. Our findings establish a unique HDAC4-MAPK-AP1 signaling axis essential for neurogenic muscle atrophy and uncover a direct crosstalk between acetylation and phosphorylation-dependent signaling cascades.

### Keywords

HDAC4; muscle atrophy; denervation; AP1; MAP kinase

### Introduction

Adult skeletal muscle is a highly adaptive tissue that can undergo changes in size, contractility, and metabolism to meet functional demands. The plasticity of myofibers reflects coordinated changes in the muscle gene expression program controlled by neural activity (Bassel-Duby and Olson, 2006). While physiological remodeling confers adaptation, pathological remodeling caused by prolonged deficits in neural input can lead to muscle atrophy. In motor neuron diseases, such as amyotrophic lateral sclerosis (ALS), denervation-associated muscle atrophy is prevalent and contributes to breathing and moving difficulty

© 2012 Elsevier Inc. All rights reserved.

#Correspondence: yao00001@mc.duke.edu.

\*These authors contributed equally to this work.

**Publisher's Disclaimer:** This is a PDF file of an unedited manuscript that has been accepted for publication. As a service to our customers we are providing this early version of the manuscript. The manuscript will undergo copyediting, typesetting, and review of the resulting proof before it is published in its final citable form. Please note that during the production process errors may be discovered which could affect the content, and all legal disclaimers that apply to the journal pertain.

and eventual death. While significant progress has been made in identifying downstream effectors in the muscle atrophy program including the ubiquitin E3 ligases, atrogin-1/MAFbx and MuRF1, (Bodine et al., 2001; Gomes et al., 2001), the signaling pathway that controls activity-dependent muscle atrophy remains poorly characterized. Such knowledge could provide insights into the development of therapeutic strategies for pathological muscle remodeling.

The protein deacetylase HDAC4 has emerged as a central component of muscle transcriptional reprogramming upon denervation. HDAC4 is robustly induced in surgically denervated muscle or in those affected by motor neuron diseases such as ALS (Cohen et al., 2007). In denervated muscle, elevated HDAC4 has a dual role: it represses muscle structural gene transcription (Cohen et al., 2009) but also induces genes involved in synapse formation and muscle atrophy (Cohen et al., 2007; Moresi et al., 2010; Tang et al., 2009). We previously showed that HDAC4 represses the Dach2 transcription repressor, resulting in the induction of the myogenin transcription factor and synaptic gene transcription (Cohen et al., 2007). Interestingly, the HDAC4-Dach2-myogenin transcriptional axis is also required for full induction of the ubiquitin E3 ligases MuRF1 and atrogin-1 that promote atrophy (Cohen et al., 2007; Macpherson et al., 2011; Moresi et al., 2010). Mechanistically, HDAC4 has been extensively characterized as a classical transcriptional co-repressor that binds and potently inhibits the master muscle transcription factor, MEF2 (McKinsey et al., 2000). Paradoxically, however, the conserved histone deacetylase domain of HDAC4 is completely dispensable for this activity (Chan et al., 2003). This finding suggests a yet to be characterized mode of deacetylase-dependent activity for HDAC4. In this context, while MEF2 is the canonical target of HDAC4 in muscle structural gene transcription (Cohen et al., 2009), how HDAC4 is connected to the muscle atrophy program remains unclear.

In this study, we show that HDAC4 activates neurogenic muscle atrophy independent of its canonical transcriptional repressor activity toward MEF2. Instead, denervation-induced HDAC4 activates the AP1 transcription factor by stimulating MAP kinase signaling. Unlike its intrinsic transcriptional repressor activity, we found that a functional deacetylase domain is obligatory for HDAC4 to activate the MAPK-AP1 axis. We show that HDAC4 binds and promotes deacetylation of a MAP3K2, MEKK2, thereby promoting MAPK-AP1 signaling and muscle atrophy. Our study identifies an HDAC4-MAP kinase-AP1 network as the critical effector in denervation-induced atrophy and uncovers a direct cross-talk between HDAC and MAP kinase signaling.

## Results

### The AP1-cytokine transcriptional network is activated by HDAC4 in denervated muscle

To unravel the mechanism by which HDAC4 promotes atrophy, we performed gene expression analysis to identify potential transcriptional targets of HDAC4 in denervated muscle. Mouse tibialis anterior (TA) muscles were transfected with control siRNA or HDAC4-specific siRNA by electroporation followed by surgical denervation for 14 days, and then subjected to morphometric or gene expression analysis. Introduction of HDAC4-specific siRNA significantly inhibited denervation-induced atrophy (Figure 1A) as was also shown previously (Moresi et al., 2010). Analysis of HDAC4 knockdown (KD) and control denervated muscles revealed the induction of many inflammatory cytokines in denervated muscle in an HDAC4-dependent manner (Figure S1A). Direct real-time RT-PCR analysis confirmed the induction of representative cytokines, *IL-6* and *IL-1beta*, in control but not HDAC4 KD denervated muscles (Figure 1B). Gene expression analysis also revealed the induction of *c-jun* and *c-fos*, key components of the AP1 transcription factor that activates inflammatory cytokine gene transcription (Adcock, 1997). Immuno-staining analysis confirmed a prominent accumulation of c-jun in denervated muscle but the induction was

lost upon KD of HDAC4 (Figure S1B). These results identify the AP1-inflammatory cytokine transcriptional program as a regulatory target of HDAC4 in denervated muscle.

Since inflammatory cytokine production has been implicated in the activation of the muscle atrophy program associated with cancer cachexia (Argiles et al., 2003; Bossola et al., 2008; Spate and Schulze, 2004), we reasoned that the AP1-dependent cytokine transcription program might be important in denervation-induced atrophy. To test this possibility, we inactivated AP1 in skeletal muscle by introducing a specific c-fos siRNA into TA muscle. As shown in Figure 2A, knockdown of c-fos effectively blunted the induction of *IL-6* and *IL-1beta* in denervated TA muscles, indicating that AP1 activates inflammatory cytokine transcription in response to denervation. Most importantly, myofibers receiving c-fos siRNA were also much more resistant to atrophy induced by denervation (Figure 2B). Consistent with this finding, the inductions of *MuRF1* and *atrogin-1* were markedly suppressed by c-fos KD (Figure 2C). Similarly, KD of c-jun also curbed the induction of ubiquitin E3 ligases (Figure S2). Interestingly, c-fos KD had no significant effect on *myogenin* expression (Figure 2C), indicating that AP1 regulates atrophy independent of myogenin induction. Together, these results demonstrate that HDAC4-dependent AP1 activity is a critical component of denervation-induced cytokine production and muscle atrophy.

### HDAC4 stimulates AP1 activity by activating the MAP kinase-signaling cascade

We next determined how HDAC4 regulates the AP1 transcription network. To recapitulate the elevated levels of HDAC4 in denervated muscle, we transfected C2C12 myoblasts with an HDAC4 expression plasmid and analyzed AP1 activity using a reporter assay. In stark contrast to its robust inhibitory activity on a MEF2 reporter, HDAC4 potently activated the AP1 reporter (> 10 fold, Figure 3A). Interestingly, HDAC5 and other class IIA HDAC members, which are also known to inhibit MEF2 (Haberland et al., 2009), did not activate the AP1 reporter (Figure S3). These results suggest that HDAC4 regulates AP1 and MEF2 activity by distinct mechanisms. Supporting this possibility, we found that the nuclear-localized HDAC4 3SA mutant, which encodes a super repressor of MEF2 (Zhao et al., 2001), was also ineffective for full activation of AP1. Importantly, while the catalytic activity of HDAC4 is completely dispensable for repressing MEF2 activity (Chan et al., 2003), the catalytically deficient HDAC4 (CAD) mutant failed to activate the AP1 reporter. Together, these results show that HDAC4 activates AP1 activity independent of its well-characterized transcriptional repressor activity but requires an intact catalytic domain.

AP1 induction and activation are regulated by the MAP kinases including Erk1/2, p38, and JNK (Eferl and Wagner, 2003). We next considered the possibility that HDAC4 might regulate AP1 by intersecting with the MAP kinase-signaling pathway. To this end, we used pharmacological inhibitors or dominant negative (DN) mutants to selectively inhibit each of the three main MAP kinases, Erk, p38, and JNK. As shown in Figure 3B–C, we found that inhibition of the MEK-Erk pathway by an MEK1/2 inhibitor U0126 or DN-MEK1 potently repressed AP1 activity induced by HDAC4, while the p38 kinase inhibitor SB202190 or DN-MKK6 had a more moderate effect. In contrast, inhibition of JNK by SP600125 or DN-JNK1 had little effect (Figures 3B and 3C). Supporting these observations, combined treatment of MEK1/2 and p38 but not JNK inhibitors completely abolished HDAC4-induced AP1 activity (Figure 3B, last two Columns). These results show that HDAC4-dependent AP1 activity requires active MEK1/2-Erk1/2 and MKK3/6-p38 MAPK signaling.

We next asked if elevated levels of HDAC4 could activate the MEK-Erk or MKK3/6-p38 kinase pathways. Using antibodies for the phosphorylated and activated form of the kinases, we found that overexpression of HDAC4 led to an increase in phospho-MEK1/2 and -Erk1/2 (Figure 4A) as well as phospho-p38 (Figures 4B and S4A) and -MKK3 (Figure S4B) indicating that both MAPK pathways were activated. Supporting this conclusion, over-

expression of HDAC4 induced c-fos Thr-325 phosphorylation (Figure 4C), which is a known target of Erk1/2 and is associated with AP1 activation (Assoian, 2002). HDAC4-CAD or 3SA mutants, which cannot activate AP1, also failed to promote MAPK phosphorylation (Figures 4A and 4B). Collectively, these results indicate that elevated levels of HDAC4 activate MAPK signaling which in turn stimulates AP1 activity.

### **MEKK2 is required for HDAC4 to activate the MAPK-AP1 signaling cascade**

The activation of MAP2Ks, including MEK1, often requires upstream kinases, MAP3Ks. There are at least 14 MAP3 kinases identified in mammalian cells (Zhang and Dong, 2005). Among MAP3 kinases, the Raf kinases are best characterized. However, pharmacological inhibition of B-Raf and C-Raf kinase had no effect on AP1 or MEK1 activation induced by HDAC4 (Figures S5A and S5B). Screening through additional MAP3K members by siRNA identified MEKK2 as a potential mediator of HDAC4 (Figure S5C). Indeed, inhibition of MEKK2 but not MEKK1, by siRNA or a dominant-negative mutant markedly suppressed HDAC4-induced AP1 and MEK1 activation (Figures 5A, 5B and S5D). Interestingly, additional inactivation of MEKK4, a MAP3K required for MKK3-p38 signaling (Abell et al., 2007) (Figure S5E) further inhibited HDAC4-induced AP1 activation (Figure 5C). Together, these results indicate that HDAC4 activates AP1 via the MAPK pathway, primarily by a MEKK2-dependent mechanism.

### **HDAC4 binds and promotes MEKK2 deacetylation**

We next determined how HDAC4 is connected with MEKK2. Since an intact HDAC4 catalytic domain is required for AP1 activation (Figure 3A), we investigated if MEKK2 is subject to acetylation. We found that MEKK2 becomes acetylated upon co-expression with the acetyltransferases CBP (Figure 6A) or P/CAF (Figure S6A). Further, MEKK2 forms a complex with HDAC4 (Figure 6B) and becomes partially deacetylated when incubated with immunoprecipitated HDAC4 (Figure 6C). Importantly, endogenous MEKK2 purified from normal TA muscles is also subject to acetylation, and this acetylation is largely lost upon denervation (Figure 6D). Supporting an important role of HDAC4 in denervation-induced MEKK2 deacetylation, knockdown of HDAC4 significantly restored MEKK2 acetylation in denervated muscles (Figures 6D and 6E). These results show that HDAC4 can bind and promote MEKK2 deacetylation.

To investigate the role of MEKK2 acetylation, we determined the acetylation sites in MEKK2 by mass spectrometry. Interestingly, the three lysine residues acetylated by both CBP and P/CAF are all localized to the catalytic domain (Table S1). Among them, Lys 385 is a conserved residue required for kinase activity (Chayama et al., 2001; Fanger et al., 1997). Mutation of Lys (K) 385 to methionine (MEKK2-K385M) reduced CBP-mediated MEKK2 acetylation, confirming that K385 is subject to acetylation (Figure 6F). Supporting these observations, MEKK2 purified from cells over-expressing CBP had lower kinase activity than MEKK2 from control cells (Figure S6B). To further assess if acetylation affects MEKK2 activity, we generated an acetylation-mimicking K385Q (glutamine) mutant MEKK2. We found that K385Q-MEKK2 is deficient in kinase activity (Figure 6G) and AP1 activation (Figure S6C). These results indicate that acetylation inhibits MEKK2 activity and HDAC4 activates MEKK2 activity by stimulating its deacetylation.

### **HDAC4-dependent MAPK signaling is required for denervation-induced muscle atrophy**

To determine if the HDAC4-MAPK-AP1 signaling cascade is indeed involved in denervation-induced atrophy, we assessed the MAPK signaling status in denervated muscle. Upon denervation, MEK1/2 and Erk phosphorylation, and c-jun and c-fos induction were observed (Figure 7A). Similarly, phospho-MEK1/2, phospho-Erk1/2, and c-jun were induced in muscles from an ALS mouse model (SOD1-G93A) suffering from denervation

and atrophy (Figure S7A). Importantly, denervation-induced MEK-Erk activation (Figure 7B) and AP1 induction (Figure 7C) were markedly inhibited in muscles expressing an HDAC4-siRNA, further supporting the notion that HDAC4 activates the MAPK-AP1 signaling cascade in response to denervation. Interestingly, MEKK2 accumulation was observed in denervated muscles (Figure 7A), which depends on HDAC4 (Figure 7B), as well as in ALS-affected muscles (Figure S7A). To determine if MEKK2 is required for muscle atrophy, we electroporated MEKK2-specific siRNA into TA muscles. As shown in Figures 7D, 7E, and S7B, MEKK2 knockdown attenuated muscle atrophy (Figures 7D and S7B) and the expression of *MuRF1* and *atrogin-1* induced by denervation (Figure 7E). The significant but partial effect of MEKK2 KD on muscle atrophy likely reflects the involvement of an additional MAP3 kinase, MEKK4 (Figures 5C and S5E). Future studies using MEKK2 and MEKK4 knockout mice would be needed to confirm their specific contribution to muscle atrophy (Guo et al., 2002). Collectively, these results demonstrate that HDAC4, the MAP kinase cascade, and the AP1 transcription factor constitute a key signaling pathway that executes the muscle atrophy program induced by loss of neural inputs.

## Discussion

In this report, we provide evidence that HDAC4 promotes neurogenic muscle atrophy, at least in part, by activating the MAPK-AP1 signaling cascade. c-jun and c-fos, the two major AP1 subunits, have long been known to be induced in denervated muscle but with no known significance (Weis, 1994). Our finding that inactivation of c-fos significantly blunted the muscle atrophy program identifies AP1 as a critical component in the execution of neurogenic muscle atrophy (Figures 2B and 2C). Interestingly, AP1 and inflammatory cytokines have been implicated in atrophy associated with cancer cachexia (Argiles et al., 2003; Moore-Carrasco et al., 2007; Moore-Carrasco et al., 2006). We suspect that AP1-dependent cytokine production might collectively contribute to pathological muscle remodeling in denervated muscle. Future experiments would be required to determine whether the HDAC4-AP1-cytokine axis is similarly involved in cancer cachexia.

Myogenin, which is transcriptionally induced upon denervation by an HDAC4-dependent mechanism (Cohen et al., 2007), was recently reported to activate *MuRF1* and *atrogin-1* transcription and muscle atrophy (Moresi et al., 2010). Interestingly, we found that AP1 inactivation blunted the induction of *MuRF1* and *atrogin-1* in denervated muscle but had little effect on *myogenin* expression (Figure 2C). These findings reveal that HDAC4 regulates muscle atrophy by two independent pathways that converge on MuRF1 and atrogen-1 transcription. This arrangement might allow for a more efficient regulation of muscle mass in response to changes in neural and muscle activity. Importantly, our results indicate that HDAC4 activates the MAPKAP1 signaling cascade independent of its canonical transcription repressor activity but requires an intact catalytic domain. It has long been recognized that the transcriptional repressor activity of HDAC4 does not require its catalytic domain (Zhao et al., 2005). Accordingly, any specific function of the conserved catalytic domain has been elusive. In fact, evidence indicates that HDAC4 and related class IIA HDAC members do not encode for classical histone deacetylases (Bottomley et al., 2008; Fischle et al., 2002; Lahm et al., 2007). It is generally thought that HDAC4 promotes deacetylation by recruiting HDAC3 (Fischle et al., 2002; Zhao et al., 2005). However, we found that HDAC3 does not activate AP1 (Figure S3) and is not required for HDAC4 to activate AP1 (data not shown). While the detailed mechanism by which HDAC4 facilitates MEKK2 deacetylation remains to be determined, the distinct mechanisms used by HDAC4 to regulate MEF2 and the MAPK-AP1 axis highlights a potential strategy to selectively inhibit HDAC4 activity without affecting critical MEF2-dependent transcriptional programs.



Such a possibility provides a rationale for selectively targeting HDAC4 catalytic domain-dependent activity in neuromuscular diseases and other related disorders.

Our data indicate that HDAC4 activates MAPK signaling, at least in part, by binding and promoting MEKK2 deacetylation. Interestingly, a bacterial acetyltransferase, VopA, was previously shown to acetylate the ATP-binding lysine residues and inactivate MKK6 kinase, thereby inhibiting MAPK signaling and host innate immune response (Trosky et al., 2007). Collectively, these findings suggest that MAP kinase acetylation is an endogenous cellular regulatory mechanism, which is hijacked by the pathogen to gain control of MAPK-dependent innate immunity. The direct HDAC4-MAP kinase crosstalk uncovered in this study not only would greatly amplify the regulatory power of protein acetylation but also expand the potential clinical applications of HDAC inhibitors in the future.

## Experimental procedures

### Cell culture/plasmids/antibodies

C2C12 myoblasts and 293T cells were cultured in 20% FBS/DMEM and 10% FBS/DMEM, respectively. Cells were maintained at 37° C in a humidified atmosphere with 5% CO<sub>2</sub>.

The HDAC4-3SA expression plasmid was generated by subcloning the coding sequence from PBJ-HDAC4-3SA into the pcDNA3 vector. Flag-HDAC4-CAD (histidines 802 and 803 replaced with lysine and leucine respectively) and HA-MEKK2-K385Q were generated by the standard protocol for PCR-mediated mutagenesis, and the constructs were confirmed by DNA sequencing. The following plasmids have been described previously: Flag-HDAC4-WT (Zhao et al., 2005), Flag-HDAC5 (Zhao et al., 2005), HA-MEK1-8E (K97M) (Mansour et al., 1994), JNK1-APF (Ke et al., 2010), MKK6-K82M (Yuasa et al., 1998), HA-MEK1-WT (Mansour et al., 1994), HA-Erk1 (from J. Kyriakis), HA-c-fos (Morimoto et al., 2007), HA-MKK3 (Molnar et al., 1997), HA-p38 (from J. Kyriakis), HA-MEKK2 (Blank et al., 1996), myc-MEKK2 (Blonska et al., 2004), HA-CBP-WT (Zhao et al., 2005), HA-CBP-CAD (LD) (Zhao et al., 2005), MEKK1-K1253M (Widmann et al., 1998), HA-MEKK2-K385M (Fanger et al., 1997), HA-MEKK4-K1361M (Gerwins et al., 1997), AP1-Luc (Ke et al., 2010), and MEF2-Luc (Zhao et al., 2001).

The following antibodies were used: p-MEK1/2, total MEK1/2, p-Erk1/2, total Erk1/2, p-p38, p-MKK3/6, pan Acetyl-K, and GAPDH antibodies from Cell Signaling; c-jun, c-fos, and MEKK4 antibodies from Santa Cruz; p-c-fos antibody from Invitrogen; MEKK2 antibody from Abcam and Santa Cruz; Flag and HA antibodies from Sigma; and myc antibody from Covance. Polyclonal anti-HDAC4 antibody was previously described (Zhao et al., 2001).

### Mouse procedures

All mice used for electroporation and denervation were on the C57BL/6 background and 6–8 weeks old (Jackson Laboratories). SOD1-G93A transgenic mice were also purchased from Jackson Laboratories. Stealth siRNA duplexed oligos were from Invitrogen.

For *in vivo* electroporation analysis, control siRNA or siRNA specific for HDAC4, c-fos, myogenin, c-jun, or MEKK2 were injected into TA muscles with a GFP plasmid included to identify electroporated fibers as described previously (Cohen et al., 2009). Mice were anesthetized with a ketamine/xylazine mixture, and siRNA was directly injected into TA muscles using a cemented MicroSyringe (Hamilton). An ECM830 electroporator (BTX) was used for all electroporations. The efficacy of siRNAs was confirmed in cells or muscles. The following siRNA sequences were used in mice or cells: HDAC4, 5'-GAGCAGCAGAGGAUCCACCAGUUA-3'; three pooled c-fos siRNAs, 5'-

CCGGCUGCACUACUUACACGUCUU-3' and 5'-UCUGUCCGUCUCUAGUGCCAACUUU-3', and 5'-GGCUGCACUACUUACACGUCUCCU-3'; three pooled myogenin siRNAs, 5'-GGGAGAAGCGCAGGCUCAAGAAAGU-3', 5'-CCUUGCUCAGCUCUCCUCAACCAGGA-3', and 5'-CAGACGCCACAAUCUGCACUCCU-3'; three pooled c-jun siRNAs, 5'-GAGAGCGGUGCCUACGGCUACAGUA-3' and 5'-UGGCACAGCUAAGCAGAAAGUCAU-3' and GCUAACGCAGCAGUUGCAAACGUUU-3'; MEKK2, 5'-GGGCACAGAGCUACCCAGAUAAUCA-3'; MEKK4, 5'-UACACUUCUGCUCUGAGGAAGGAGG-3'.

For surgical denervation experiment, mice were anesthetized, the sciatic nerve was exposed, and a ~5mm piece was excised as described previously (Cohen et al., 2007). Denervation was confirmed by the loss of nerves when muscles were isolated. Mice were sacrificed by CO<sub>2</sub> euthanasia. All mice were housed at the Duke University mouse facilities in accordance with the Institutional Animal Care and Use Committee.

### Immunostaining and morphometric analysis

Cells transfected by Flag-HDAC4-WT or Flag-HDAC4-3SA were fixed in 3.7% formaldehyde in PBS and then permeabilized with 0.1% Triton X-100 in PBS for 5 min at room temperature. Cells were blocked with 5% normal goat serum in PBS and incubated with anti-p-p38 antibody, followed by Alexa Fluor 488 goat anti-rabbit IgG. HDAC4 was detected by subsequent staining using anti-Flag antibody. Nuclei were identified using Hoechst dye. Immunofluorescence images were obtained using a Zeiss Axioskop compound microscope (Carl Zeiss).

Muscle staining was performed as described previously (Cohen et al., 2009). TA muscles were frozen in methylbutane chilled in liquid nitrogen. Cryosections were stained with dystrophin antibody (NCL-DYS1) to mark muscle fibers and GFP antibody to identify the transfected fibers. The cross sectional area of approximately 200 GFP-positive muscle fibers was quantified using ImageJ software (NIH). Values were plotted and expressed as percent of fibers at a given cross-sectional area.

### Luciferase assay

The luciferase reporter assay was performed as described previously (Cohen et al., 2009). Briefly, C2C12 cells were plated at 1,500 cells/well in a 24-well plate. Each AP1 or MEF2 reporter was co-transfected with renilla reporter in combination with the plasmids by using Lipofectamine LTX and Plus reagent (Invitrogen). Cells were lysed with passive lysis buffer (Promega) at 36–48 h post-transfection unless otherwise mentioned and luciferase assays were performed using the dual luciferase reporter assay kit (Promega). Each experiment was performed in triplicate. For pharmacological inhibition, at 16 h post-transfection cells were treated with the inhibitors for additional 12 h at a concentration indicated in the figure legends.

### Gene expression and RNA analysis

RNA extraction and real-time RT-PCR were performed as described previously (Cohen et al., 2007). Superarray analysis was performed with samples obtained from TA muscles according to manufacturer's protocol (SABiosciences). TA muscles were dounce homogenized in TRIzol reagent (Invitrogen) on ice and RNA was isolated by a standard method. cDNA synthesis was carried out with oligo dT primer and an Improm II reverse transcription system (Promega) according to manufacturer's instructions. Real time RT-PCR

was performed using iQ SYBR supermix on the iCycler iQ detection system (Bio-Rad). All values were normalized to either actin or GAPDH and were expressed as fold changes versus levels measured in control samples. RT-PCR primer sequences were as follows: MuRF1, 5'-AGGTGAAGGAGGAGCTGAGTC-3' and 5'-CATGTTCTCAAAGCCTTGCTC-3'; atrogin-1, 5'-TATGCACACTGGTGCAGAGAG-3' and 5'-GTTGTCGTGTGCTGGGATTAT-3'; myogenin, 5'-GCAGGCTCAAGAAAGTGAATG-3' and 5'-CACTTAAAAGCCCCCTGCTAC-3'; c-jun, 5'-CGCACAGCCCAGGCTAAC-3' and 5'-TGAGGGCATCGTCGTAGAA-3'; c-fos, 5'-AGAGCGGAATGGTGAAG-3' and 5'-GGATTCTCCGTTTCTCTTCC-3'; IL-6, 5'-TCAATCCAGAAACCGCTATGA-3' and 5'-CACCAGCATCAGTCCCAAGA-3'; IL-1beta, 5'-CGTGCTGTCGGACCCATATGAG-3' and 5'-GCCAAGGCCACAGGTATTT-3'; HDAC4, 5'-AGCCTCAGAACGGTGGTTAT-3' and 5'-GCTGTGGATGTCCATCACTTT-3'; MEKK2, 5'-TTGTCTTTAAGCAGCCCTGAA-3' and 5'-AAAAGTCTTCCGACCGTCATT-3'; actin, 5'-ACCCAGGCATTGCTGACAGGATGC-3' and 5'-CCATCTAGAAGCATTTGCGGTGGACG-3'; GAPDH, 5'-ACAACCTTGGCATTGTGGAAG-3' and 5'-GTTGAAGTCGCAGGAGACAAC-3'.

### Western blot analysis, immunoprecipitation and *In vitro* kinase assay

Western blotting was performed as described previously (Cohen et al., 2007). For cell culture, C2C12 cells were washed with PBS twice and then lysed in extraction buffer (50 mM Tris-Cl, pH 7.4, 150 mM NaCl, 1 mM EDTA, 1% NP-40, 0.5% sodium deoxycholate, 1 mM sodium orthovanadate, 1 mM sodium fluoride, 1 mM PMSF, 0.2 mM leupeptin, protease inhibitor cocktail (Sigma)) on ice for 30 min. Lysates were cleared by centrifugation (13000 rpm for 20 min). Protein concentrations were determined using BCA assay (Pierce). Equal amounts of cell extracts were then resolved by SDS-PAGE, transferred to nitrocellulose membranes, and probed with antibodies. Blots were detected using an ECL system (Amersham). For muscle samples, isolated TA muscles were stored in liquid nitrogen. Muscles were homogenized by glass-to-glass dounce homogenizer in suspension buffer (50 mM NaCl, 20 mM Tris, pH 7.4, 1 mM EDTA, 1 mM DTT, 1 mM sodium orthovanadate, 1 mM sodium fluoride, 1 mM PMSF, 0.2 mM leupeptin, protease inhibitor cocktail). Detergents were added to the muscle lysate (final detergent concentration: 1% NP-40, 0.5% sodium deoxycholate, 0.1% SDS) and lysates were incubated for 20 min rocking at 4° C. Lysates were cleared by centrifugation (13000 rpm for 20 min).

For immunoprecipitation, 293T cells or C2C12 myoblasts were lysed in NETN buffer (50 mM Tris-Cl, pH 7.4, 150 mM NaCl, 1 mM EDTA, 1% NP-40, 1 mM sodium orthovanadate, 1 mM sodium fluoride, 1 mM PMSF, 0.2 mM leupeptin, protease inhibitor cocktail). Cleared supernatants by centrifugation were incubated overnight with each antibody indicated in the figure legends. For detection of MEKK2 acetylation, TA muscles were homogenized and lysed by muscle lysis condition described above and lysates were immunoprecipitated with MEKK2 antibody (Abcam). Immunoprecipitated products were analyzed by Western blotting.

Kinase assay was performed as previously described (Blank et al., 1996) with slight modifications. Briefly, 293T cells were transfected with HA-MEKK2-WT or -K385Q and then lysed in NETN buffer. Whole cell lysates were immunoprecipitated with HA-agarose beads overnight. Immunoprecipitates were washed 3 times with NETN buffer and twice with buffer containing 10 mM Pipes, pH 7.0, 100 mM NaCl. Beads were then incubated with purified HA-MEK1-K97M protein in kinase buffer (20 mM Pipes, 10 mM MnCl<sub>2</sub>) containing 60 – 120 μM ATP for 30 min at 30°C. Reactions were terminated by adding 2X sample buffer and samples were analyzed for MEK phosphorylation by immunoblotting. Additionally, to purify non-acetylated and acetylated forms of MEKK2, myc-MEKK2 was



co-transfected with/without HA-CBP into 293T cells. Immunoprecipitated MEKK2 with myc antibody was purified by adding myc-peptide (Sigma), according to the manufacturer's instructions. The kinase assay was performed as described above.

### ***In vitro* deacetylation assay**

293T cells were transfected with two sets of plasmids in 10 cm plates. One set contained pcDNA-myc-MEKK2 and pcDNA-HA-CBP. The other set contained pcDNA-Flag-HDAC4. Cells were harvested 24 h after transfection. Cells were resuspended and incubated in 400  $\mu$ l of low stringency buffer (50 mM Tris-Cl, pH 7.6, 120 mM NaCl, 0.5 mM EDTA, 0.5% NP-40) with protease inhibitors for 30 min. Lysates were cleared by centrifugation at 14K RPM for 10 min. MEKK2 and HDAC4 were pulled down by anti-myc and -Flag antibodies, respectively. After immunoprecipitation (IP) with each antibody for 3 h, 50  $\mu$ l of protein A beads (50% slurry) was added into the IP mixture and incubated for another 4 h. Then the beads were washed 3 times in 1 ml Low Stringency Buffer and 2 times in 1 ml High Stringency Buffer (50 mM Tris-Cl, pH 7.6, 500 mM NaCl, 0.5 mM EDTA, 0.5% NP-40) and finally washed 2 times in 1 ml HDAC buffer (10 mM Tris-Cl, pH 8.0, 10 mM NaCl, 10% glycerol). Beads with myc-MEKK2 and Flag-HDAC4 were resuspended in 40  $\mu$ l HDAC Buffer, mixed together, and incubated at 37° C on rocker for 4 h. Proteins were eluted by adding 10  $\mu$ l of 4X SDS sample buffer and heating for 3 min. The supernatant was subjected to SDS-PAGE for Western blot analysis. Acetylation of MEKK2 was detected by anti-acetyl lysine (Ac-K) antibody.

### **Identification of acetylation sites in MEKK2**

Large-scale transfection was performed in 293T cells. Myc-MEKK2 was co-expressed with HA-CBP or Flag-P/CAF and cells were lysed by the buffer used for Western blot analysis. Immunoprecipitated MEKK2 with anti-myc antibody was loaded for SDS-PAGE. Following coomassie staining/destaining (Bio-Rad), bands corresponding to MEKK2 were excised from gel.

For in-gel tryptic digestion, the gel bands were washed with 50% ethanol for 1 h, and then again overnight. The destained gel bands were washed with deionized water twice and then were cut into small cubic pieces of about 1 mm. The gel pieces were reduced with 10 mM dithiothreitol (Sigma) at 56° C for 1 h and then alkylated with 55 mM iodoacetamide (Sigma) at room temperature in the dark for 45 min. Enzymatic digestion was done by adding trypsin (Promega) in 50 mM ammonium bicarbonate to the gel pieces, followed by overnight-incubation at 37° C and 50% acetonitrile in 5% trifluoroacetic acid (TFA) and 75% acetonitrile in 1% TFA were sequentially added to the gel pieces for the extraction of tryptic peptides. The pooled extracts were dried in a SpeedVAc, desalted with a  $\mu$ -C18 ZipTip (Millipore), and then dried again prior to HPLC/MS/MS analysis

For HPLC-MS/MS analysis and database searching, peptide mixtures were analyzed by LC-MS/MS using an Eksigent NanoLC-1Dplus HPLC system (Eksigent Technologies) interfaced to an LTQ-Orbitrap Discovery instrument (ThermoFisher Scientific). The nanoliter flow LC instrument was operated with a 10-cm analytical column (75- $\mu$ m inner diameter, 350- $\mu$ m outer diameter) packed with Jupiter C<sub>12</sub> resin (4- $\mu$ m particle size, 90-Å pore size, Phenomenex). Solvent A was 0.1% formic acid in ddH<sub>2</sub>O, and solvent B was 100% acetonitrile (Fisher Scientific) with 0.1% formic acid. Peptide samples were injected in solvent A and were separated with a gradient of 10–90% solvent B over 40 min at a flow rate of 500 nl/min. The nanoelectrospray ion source was used with a spray voltage of 1.8 kV. No sheath, sweep, or auxiliary gasses were used, and capillary temperature was set to 180° C. The mass spectrometer was operated in a data-dependent mode to automatically switch between MS and MS/MS acquisition. Survey full-scan MS spectra (from *m/z* 350–

1,500) were acquired in the Orbitrap with resolution  $R = 30,000$  at  $m/z$  400. The ten most intense ions, with singly charged precursor ions excluded, were sequentially isolated in the linear ion trap and subjected to collision induced dissociation (CID) with a normalized energy of 35%. The following MS/MS scan was used: (1) exclusion duration for the data-dependant scan: 36 sec, (2) repeat count: 2, (3) exclusion window: +2 and -1 Da. The acquired data were analyzed by Mascot (v2.1, Matrix Science). Precursor mass tolerance for Mascot analysis was set at  $\pm 2$  Da, and fragment mass tolerance was set at  $\pm 0.5$  Da. The DB searching of all data was done with the National Center for Biotechnology Information nonredundant *Mus musculus* database. Cysteine alkylation by iodoacetamide, methione oxidation and lysine acetylation were specified as variable modifications.

## Supplementary Material

Refer to Web version on PubMed Central for supplementary material.

## Acknowledgments

We thank Ms. A. McClure and Dr. B. Mathey-Prevot for critically reading the manuscript. We also thank Dr. Natalie G. Ahn (MKK1-wt, MKK1-8E), Eisuke Nishida (HA-c-fos), Xin Lin (myc-MEKK2), and Jennifer Y. Zhang (JNK1 DN, AP1-luc) for kindly providing constructs. This work was supported by CA126832 (NCI) to Y.M.Z. and AR055613 (NIAMS, NIH) to T.P.Y. This work was also supported in part by the National Research Foundation of Korea Grant funded by the Korean Government [NRF-2009-352-C00137].

## References

- Abell AN, Granger DA, Johnson GL. MEKK4 stimulation of p38 and JNK activity is negatively regulated by GSK3beta. *J Biol Chem.* 2007; 282:30476–30484. [PubMed: 17726008]
- Adcock IM. Transcription factors as activators of gene transcription: AP-1 and NF-kappa B. *Monaldi Arch Chest Dis.* 1997; 52:178–186. [PubMed: 9203818]
- Argiles JM, Busquets S, Lopez-Soriano FJ. Cytokines in the pathogenesis of cancer cachexia. *Curr Opin Clin Nutr Metab Care.* 2003; 6:401–406. [PubMed: 12806213]
- Assoian RK. Common sense signalling. *Nat Cell Biol.* 2002; 4:E187–E188. [PubMed: 12149626]
- Bassel-Duby R, Olson EN. Signaling pathways in skeletal muscle remodeling. *Annu Rev Biochem.* 2006; 75:19–37. [PubMed: 16756483]
- Blank JL, Gerwins P, Elliott EM, Sather S, Johnson GL. Molecular cloning of mitogen-activated protein/ERK kinase kinases (MEKK) 2 and 3. Regulation of sequential phosphorylation pathways involving mitogen-activated protein kinase and c-Jun kinase. *J Biol Chem.* 1996; 271:5361–5368. [PubMed: 8621389]
- Blonska M, You Y, Geleziunas R, Lin X. Restoration of NF-kappaB activation by tumor necrosis factor alpha receptor complex-targeted MEKK3 in receptor-interacting protein-deficient cells. *Mol Cell Biol.* 2004; 24:10757–10765. [PubMed: 15572679]
- Bodine SC, Latres E, Baumhueter S, Lai VK, Nunez L, Clarke BA, Poueymirou WT, Panaro FJ, Na E, Dharmarajan K, et al. Identification of ubiquitin ligases required for skeletal muscle atrophy. *Science.* 2001; 294:1704–1708. [PubMed: 11679633]
- Bossola M, Pacelli F, Tortorelli A, Rosa F, Doglietto GB. Skeletal muscle in cancer cachexia: the ideal target of drug therapy. *Curr Cancer Drug Targets.* 2008; 8:285–298. [PubMed: 18537552]
- Bottomley MJ, Lo Surdo P, Di Giovine P, Cirillo A, Scarpelli R, Ferrigno F, Jones P, Neddermann P, De Francesco R, Steinkuhler C, et al. Structural and functional analysis of the human HDAC4 catalytic domain reveals a regulatory structural zinc-binding domain. *J Biol Chem.* 2008; 283:26694–26704. [PubMed: 18614528]
- Chan JK, Sun L, Yang XJ, Zhu G, Wu Z. Functional characterization of an amino-terminal region of HDAC4 that possesses MEF2 binding and transcriptional repressive activity. *J Biol Chem.* 2003; 278:23515–23521. [PubMed: 12709441]
- Chayama K, Papst PJ, Garrington TP, Pratt JC, Ishizuka T, Webb S, Ganiatsas S, Zon LI, Sun W, Johnson GL, et al. Role of MEKK2-MEK5 in the regulation of TNF-alpha gene expression and

- MEKK2-MKK7 in the activation of c-Jun N-terminal kinase in mast cells. *Proc Natl Acad Sci U S A*. 2001; 98:4599–4604. [PubMed: 11274363]
- Cohen TJ, Barrientos T, Hartman ZC, Garvey SM, Cox GA, Yao TP. The deacetylase HDAC4 controls myocyte enhancing factor-2-dependent structural gene expression in response to neural activity. *Faseb J*. 2009; 23:99–106. [PubMed: 18780762]
- Cohen TJ, Waddell DS, Barrientos T, Lu Z, Feng G, Cox GA, Bodine SC, Yao TP. The histone deacetylase HDAC4 connects neural activity to muscle transcriptional reprogramming. *J Biol Chem*. 2007; 282:33752–33759. [PubMed: 17873280]
- Eferl R, Wagner EF. AP-1: a double-edged sword in tumorigenesis. *Nat Rev Cancer*. 2003; 3:859–868. [PubMed: 14668816]
- Fanger GR, Johnson NL, Johnson GL. MEK kinases are regulated by EGF and selectively interact with Rac/Cdc42. *Embo J*. 1997; 16:4961–4972. [PubMed: 9305638]
- Fischle W, Dequiedt F, Hendzel MJ, Guenther MG, Lazar MA, Voelter W, Verdin E. Enzymatic activity associated with class II HDACs is dependent on a multiprotein complex containing HDAC3 and SMRT/N-CoR. *Mol Cell*. 2002; 9:45–57. [PubMed: 11804585]
- Gerwins P, Blank JL, Johnson GL. Cloning of a novel mitogen-activated protein kinase kinase kinase, MEKK4, that selectively regulates the c-Jun amino terminal kinase pathway. *J Biol Chem*. 1997; 272:8288–8295. [PubMed: 9079650]
- Gomes MD, Lecker SH, Jagoe RT, Navon A, Goldberg AL. Atrogin-1, a muscle-specific F-box protein highly expressed during muscle atrophy. *Proc Natl Acad Sci U S A*. 2001; 98:14440–14445. [PubMed: 11717410]
- Guo Z, Clydesdale G, Cheng J, Kim K, Gan L, McConkey DJ, Ullrich SE, Zhuang Y, Su B. Disruption of Mekk2 in mice reveals an unexpected role for MEKK2 in modulating T-cell receptor signal transduction. *Mol Cell Biol*. 2002; 22:5761–5768. [PubMed: 12138187]
- Haberland M, Montgomery RL, Olson EN. The many roles of histone deacetylases in development and physiology: implications for disease and therapy. *Nat Rev Genet*. 2009; 10:32–42. [PubMed: 19065135]
- Ke H, Harris R, Coloff JL, Jin JY, Leshin B, Miliani de Marval P, Tao S, Rathmell JC, Hall RP, Zhang JY. The c-Jun NH2-terminal kinase 2 plays a dominant role in human epidermal neoplasia. *Cancer Res*. 2010; 70:3080–3088. [PubMed: 20354187]
- Lahm A, Paolini C, Pallaoro M, Nardi MC, Jones P, Neddermann P, Sambucini S, Bottomley MJ, Lo Surdo P, Carfi A, et al. Unraveling the hidden catalytic activity of vertebrate class IIa histone deacetylases. *Proc Natl Acad Sci U S A*. 2007; 104:17335–17340. [PubMed: 17956988]
- Macpherson PC, Wang X, Goldman D. Myogenin regulates denervation-dependent muscle atrophy in mouse soleus muscle. *J Cell Biochem*. 2011
- Mansour SJ, Matten WT, Hermann AS, Candia JM, Rong S, Fukasawa K, Vande Woude GF, Ahn NG. Transformation of mammalian cells by constitutively active MAP kinase kinase. *Science*. 1994; 265:966–970. [PubMed: 8052857]
- McKinsey TA, Zhang CL, Lu J, Olson EN. Signal-dependent nuclear export of a histone deacetylase regulates muscle differentiation. *Nature*. 2000; 408:106–111. [PubMed: 11081517]
- Molnar A, Theodoras AM, Zon LI, Kyriakis JM. Cdc42Hs, but not Rac1, inhibits serum-stimulated cell cycle progression at G1/S through a mechanism requiring p38/RK. *J Biol Chem*. 1997; 272:13229–13235. [PubMed: 9148940]
- Moore-Carrasco R, Busquets S, Almendro V, Palanki M, Lopez-Soriano FJ, Argiles JM. The AP-1/NF-kappaB double inhibitor SP100030 can revert muscle wasting during experimental cancer cachexia. *Int J Oncol*. 2007; 30:1239–1245. [PubMed: 17390027]
- Moore-Carrasco R, Garcia-Martinez C, Busquets S, Ametller E, Barreiro E, Lopez-Soriano FJ, Argiles JM. The AP-1/CJUN signaling cascade is involved in muscle differentiation: implications in muscle wasting during cancer cachexia. *FEBS Lett*. 2006; 580:691–696. [PubMed: 16412434]
- Moresi V, Williams AH, Meadows E, Flynn JM, Potthoff MJ, McAnally J, Shelton JM, Backs J, Klein WH, Richardson JA, et al. Myogenin and class II HDACs control neurogenic muscle atrophy by inducing E3 ubiquitin ligases. *Cell*. 2010; 143:35–45. [PubMed: 20887891]

- Morimoto H, Kondoh K, Nishimoto S, Terasawa K, Nishida E. Activation of a C-terminal transcriptional activation domain of ERK5 by autophosphorylation. *J Biol Chem.* 2007; 282:35449–35456. [PubMed: 17928297]
- Spate U, Schulze PC. Proinflammatory cytokines and skeletal muscle. *Curr Opin Clin Nutr Metab Care.* 2004; 7:265–269. [PubMed: 15075917]
- Tang H, Macpherson P, Marvin M, Meadows E, Klein WH, Yang XJ, Goldman D. A histone deacetylase 4/myogenin positive feedback loop coordinates denervation-dependent gene induction and suppression. *Mol Biol Cell.* 2009; 20:1120–1131. [PubMed: 19109424]
- Trosky JE, Li Y, Mukherjee S, Keitany G, Ball H, Orth K. VopA inhibits ATP binding by acetylating the catalytic loop of MAPK kinases. *J Biol Chem.* 2007; 282:34299–34305. [PubMed: 17881352]
- Weis J. Jun, Fos, MyoD1, and myogenin proteins are increased in skeletal muscle fiber nuclei after denervation. *Acta Neuropathol.* 1994; 87:63–70. [PubMed: 8140895]
- Widmann C, Gerwins P, Johnson NL, Jarpe MB, Johnson GL. MEK kinase 1, a substrate for DEVD-directed caspases, is involved in genotoxin-induced apoptosis. *Mol Cell Biol.* 1998; 18:2416–2429. [PubMed: 9528810]
- Yuasa T, Ohno S, Kehrl JH, Kyriakis JM. Tumor necrosis factor signaling to stress-activated protein kinase (SAPK)/Jun NH2-terminal kinase (JNK) and p38. Germinal center kinase couples TRAF2 to mitogen-activated protein kinase/ERK kinase 1 and SAPK while receptor interacting protein associates with a mitogen-activated protein kinase kinase upstream of MKK6 and p38. *J Biol Chem.* 1998; 273:22681–22692. [PubMed: 9712898]
- Zhang YL, Dong C. MAP kinases in immune responses. *Cell Mol Immunol.* 2005; 2:20–27. [PubMed: 16212907]
- Zhao X, Ito A, Kane CD, Liao TS, Bolger TA, Lemrow SM, Means AR, Yao TP. The modular nature of histone deacetylase HDAC4 confers phosphorylation-dependent intracellular trafficking. *J Biol Chem.* 2001; 276:35042–35048. [PubMed: 11470791]
- Zhao X, Sternsdorf T, Bolger TA, Evans RM, Yao TP. Regulation of MEF2 by histone deacetylase 4- and SIRT1 deacetylase-mediated lysine modifications. *Mol Cell Biol.* 2005; 25:8456–8464. [PubMed: 16166628]

### Highlights

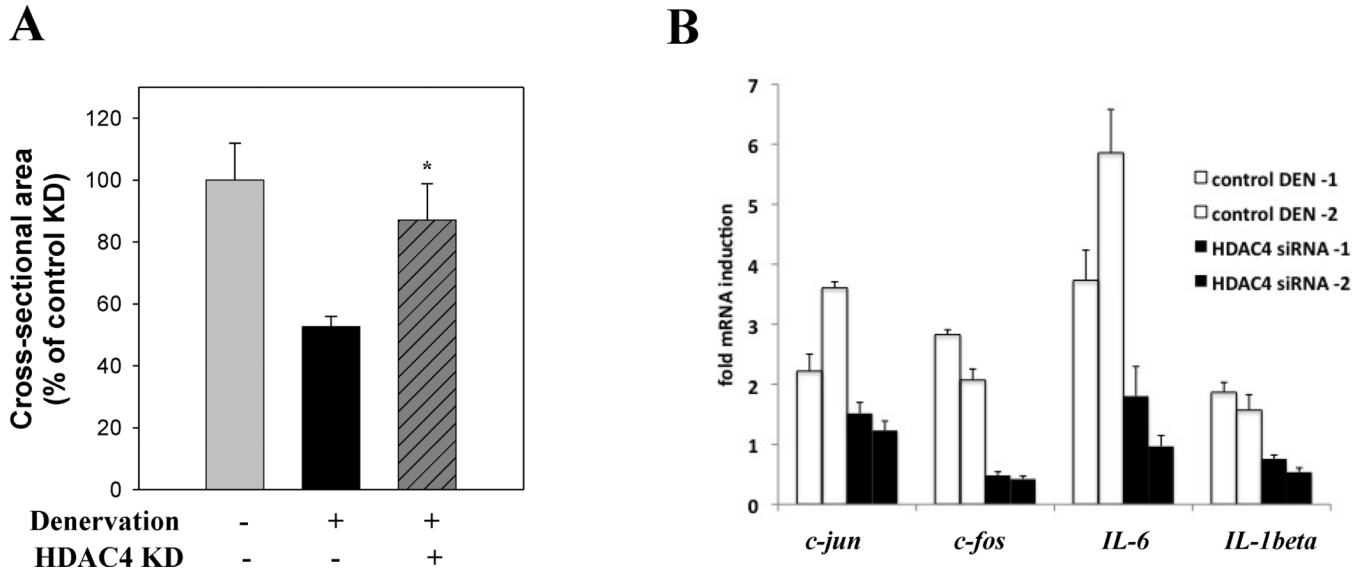
HDAC4 targets the AP1 but not MEF2 transcription program in neurogenic muscle atrophy.

HDAC4 stimulates AP1 activity by activating MAP kinase signaling.

HDAC4 activates the MAPK cascade by promoting the deacetylation an MAP3K, MEKK2.

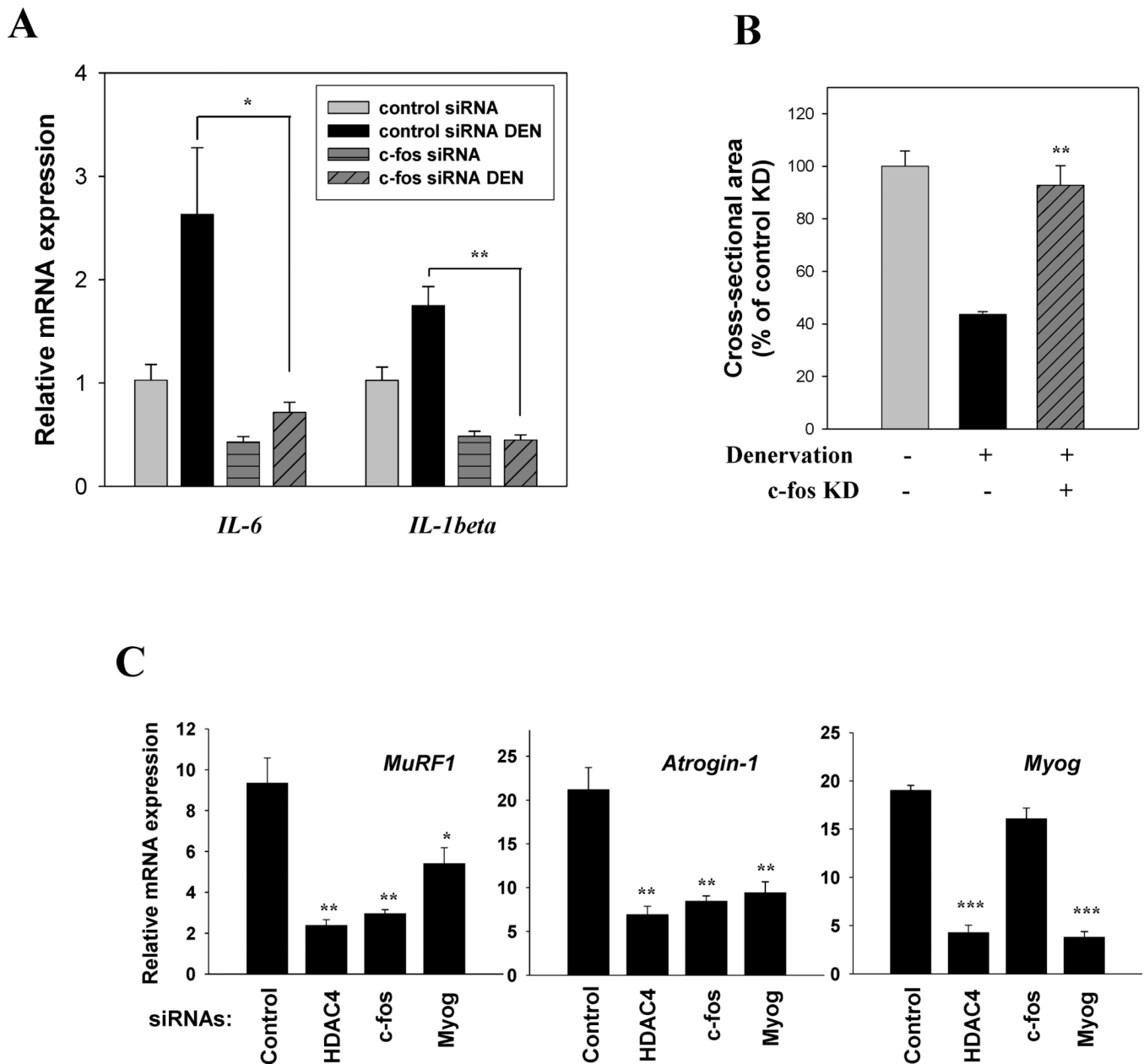
The HDAC4-MAPK-AP1 signaling cascade is essential for neurogenic muscle atrophy.





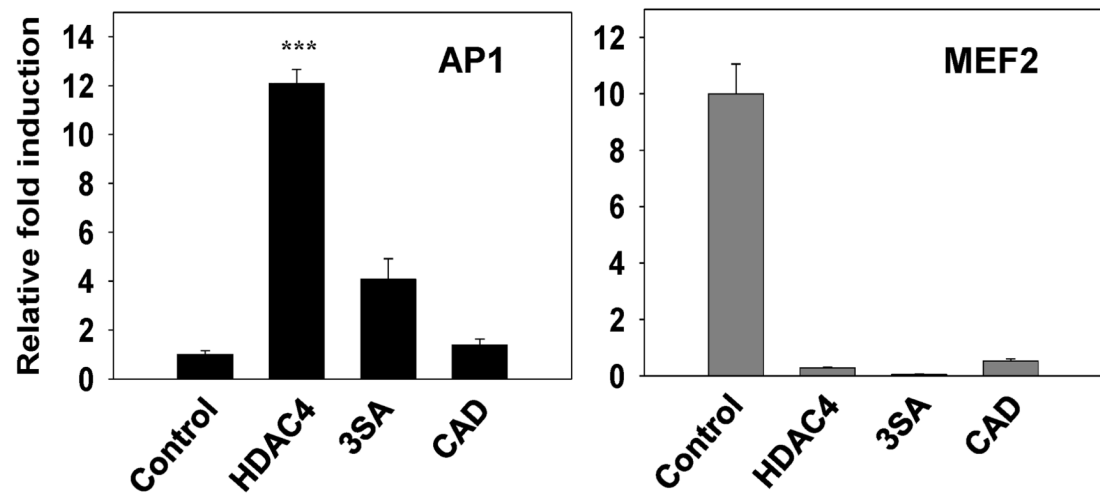
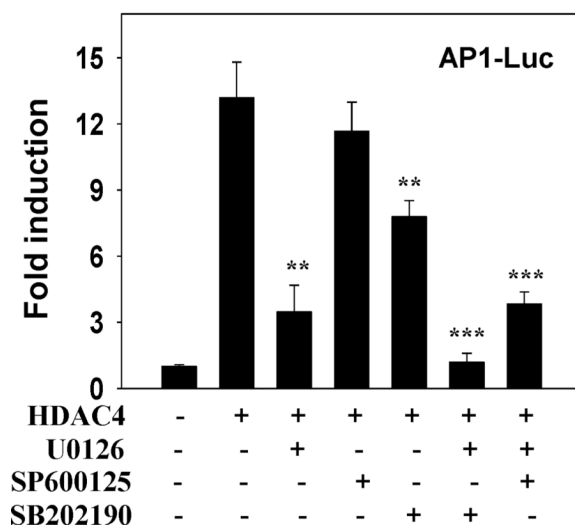
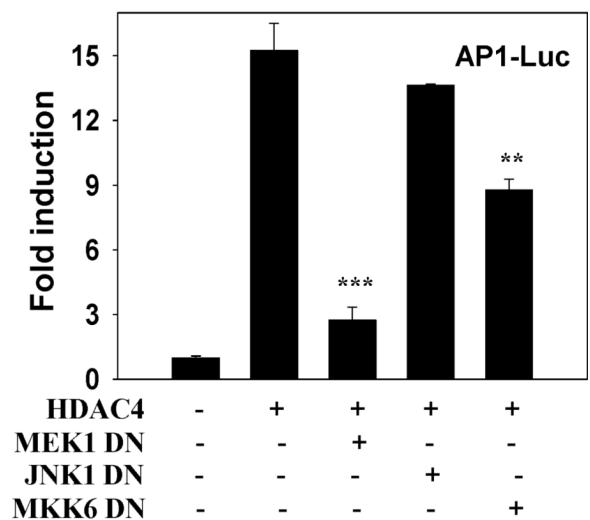
**Figure 1.**

HDAC4 is required for denervation-induced muscle atrophy and AP1-cytokines expression. (A) Quantification of mean fiber CSA (cross-sectional area) in TA muscle of control KD, control KD-denervated, and HDAC4 KD-denervated mice 14 days after denervation. Values are expressed as percentage of control KD ( $n = 3$  for each group). \* $P < 0.05$  versus control KD-denervated (unpaired Student's  $t$ -test). (B) Expressions of inflammatory cytokines and AP1 in denervated muscle mediated by HDAC4. The fold induction of *c-jun*, *c-fos*, *IL-6* and *IL-1beta* mRNA 14 days after denervation was determined in control or HDAC4-siRNA transfected TA muscle by real-time RT-PCR. Values were normalized to actin. Error bars were generated from real-time PCR triplicates and represent SD ( $n = 2$  per group).



**Figure 2.** The AP1 transcription factor regulated by HDAC4 is critical for denervation-induced muscle atrophy and cytokine expression. (A) Expressions of *IL-6* and *IL-1beta* were detected by real-time RT-PCR in TA muscle electroporated with control or c-fos siRNA and denervated for 14 days. Values were normalized to actin. Columns, mean ( $n = 3$  for each group); bars, SEM. \* $P < 0.05$ , \*\* $P < 0.01$  versus control siRNA DEN (unpaired Student's *t*-test). (B) Mean fiber CSA was quantified to determine fiber size in TA muscle of control KD, control KD-denervated, and c-fos KD-denervated mice 14 days after denervation. Values are expressed as percentage of control KD ( $n = 3$  for each group). \*\* $P < 0.01$  versus control KD-denervated (unpaired Student's *t*-test). (C) Expressions of *MuRF1*, *atrogin-1*, and *myogenin* were determined by real-time RT-PCR in TA muscles that were electroporated with control, HDAC4, c-fos or myogenin siRNA and denervated for 7 days. Values were

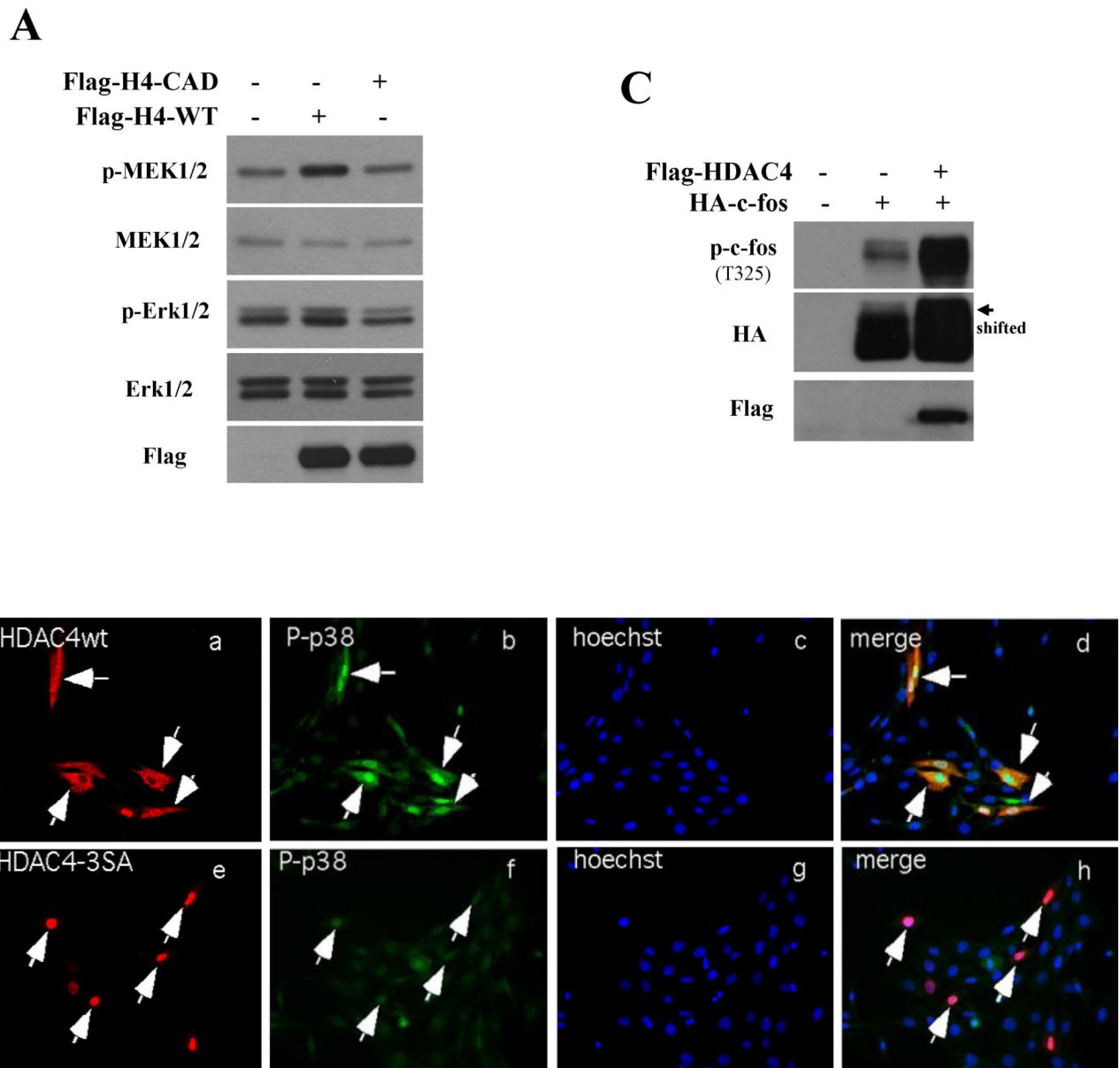
normalized to GAPDH. Relative fold change was calculated compared to control siRNA non-DEN. Columns, mean; bars, SEM.  $n = 4$  for each group. \* $P < 0.05$ , \*\* $P < 0.01$ , \*\*\* $P < 0.001$  versus control siRNA DEN (unpaired Student's  $t$ -test).

**A****B****C****Figure 3.**

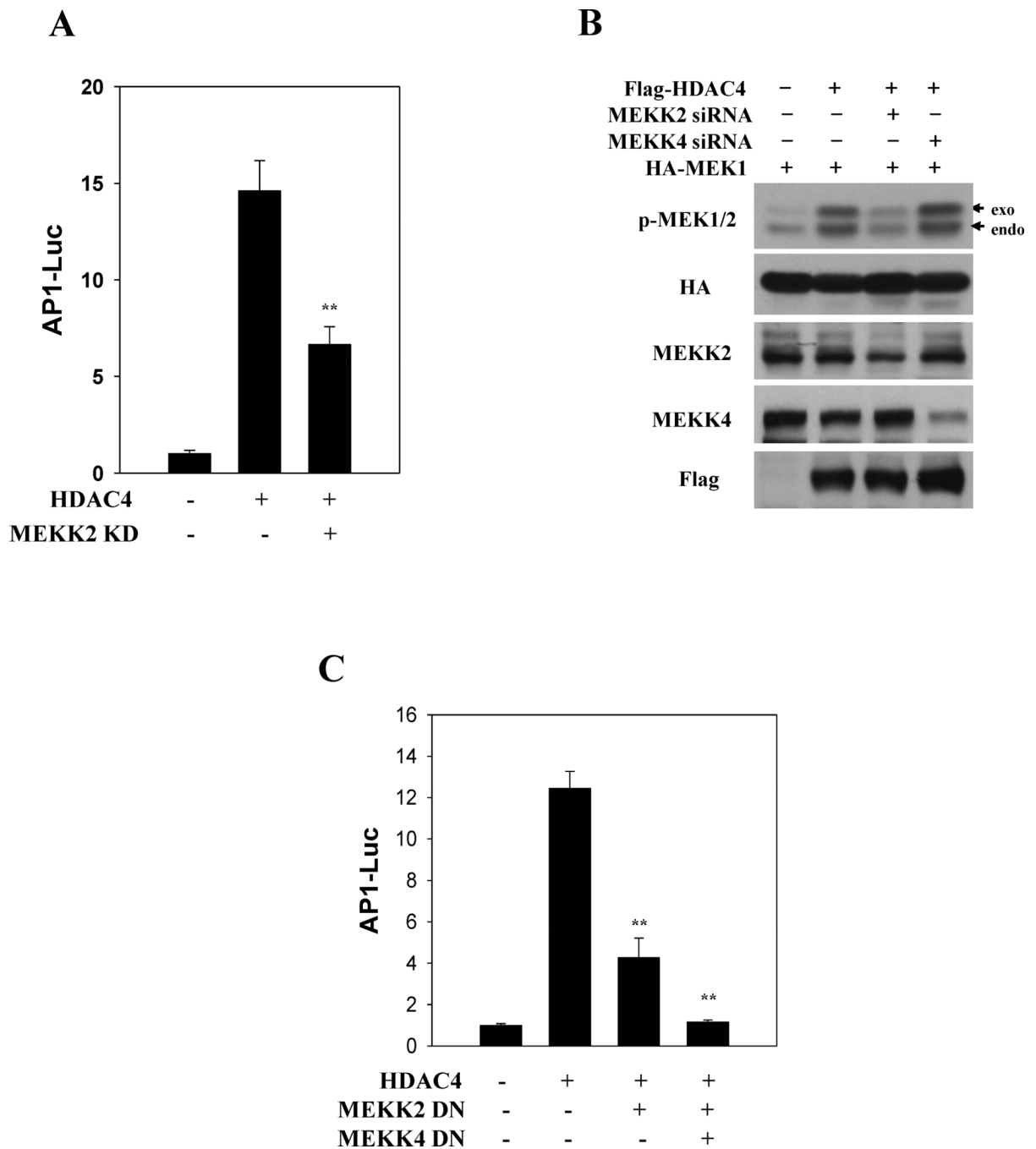
HDAC4 activates AP1 by a MAPK-dependent but MEF2-independent mechanism. (A) AP1 activation by HDAC4. AP1 (*left* panel) or MEF2 reporter (*right* panel) activity was measured in C2C12 myoblasts transfected with an expression plasmid of HDAC4 WT, nuclear localized mutant (3SA), or catalytically dead mutant (CAD, histidines 802 and 803 replaced with lysine and leucine respectively). Columns, mean; Bars, SD ( $n = 3$ ). \*\*\* $P < 0.001$  versus control. (B) C2C12 cells were co-transfected with HDAC4 and an AP1 reporter and subsequently treated with inhibitors for MEK1/2 (U0126, 10 $\mu$ M), JNK (SP600125, 10 $\mu$ M), p38 (SB202190, 20 $\mu$ M). Lysates were then subjected to the luciferase reporter assay. Columns, mean; Bars, SD ( $n = 3$ ). \*\* $P < 0.01$ , \*\*\* $P < 0.001$  versus HDAC4 overexpression with no treatment. (C) Effect of dominant negative (DN) mutants against

MAP kinase pathway on HDAC4-induced AP1 activation. Columns, mean; Bars, SD ( $n = 3$ ). \*\*\* $P < 0.001$  versus HDAC4 overexpression.

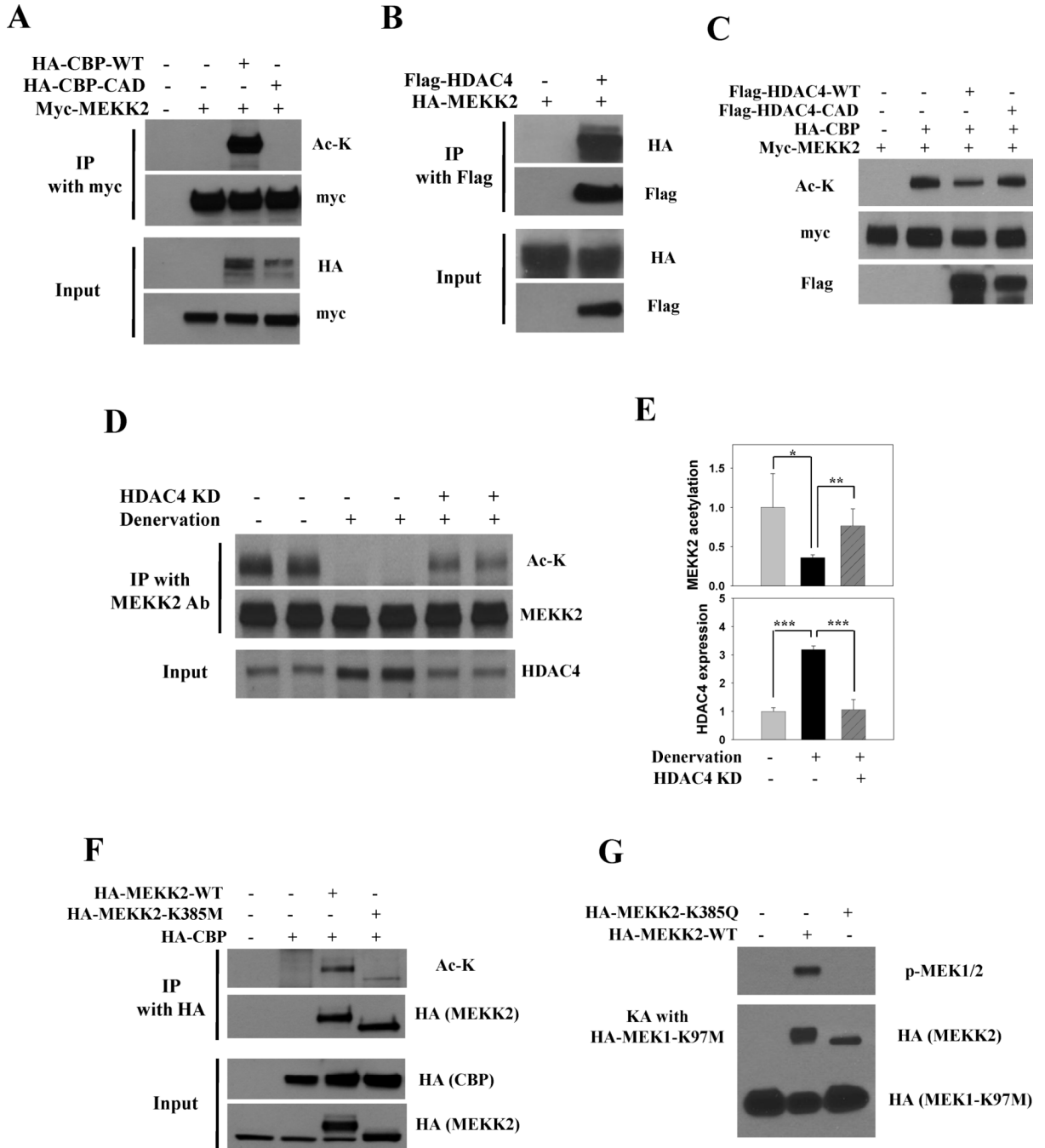




**Figure 4.** Activation of MAP kinase signaling by HDAC4. (A) Flag-tagged HDAC4 wild type (WT) or catalytically dead mutant (CAD) was transfected into C2C12 myoblasts with equal amount of expression, and lysates were subjected to western blotting using p-MEK1/2 and p-Erk1/2 antibodies. (B) Activation of endogenous p38 by HDAC4. Cells were transfected with Flag-HDAC4 and stained with anti-Flag antibody (red) and anti-phospho-p38 antibody (green). DNA (blue) was visualized by Hoechst staining. (C) Flag-tagged HDAC4 was co-transfected into C2C12 myoblasts with HA-c-fos, and activation of c-fos was detected using p-c-fos (Thr325) antibody.

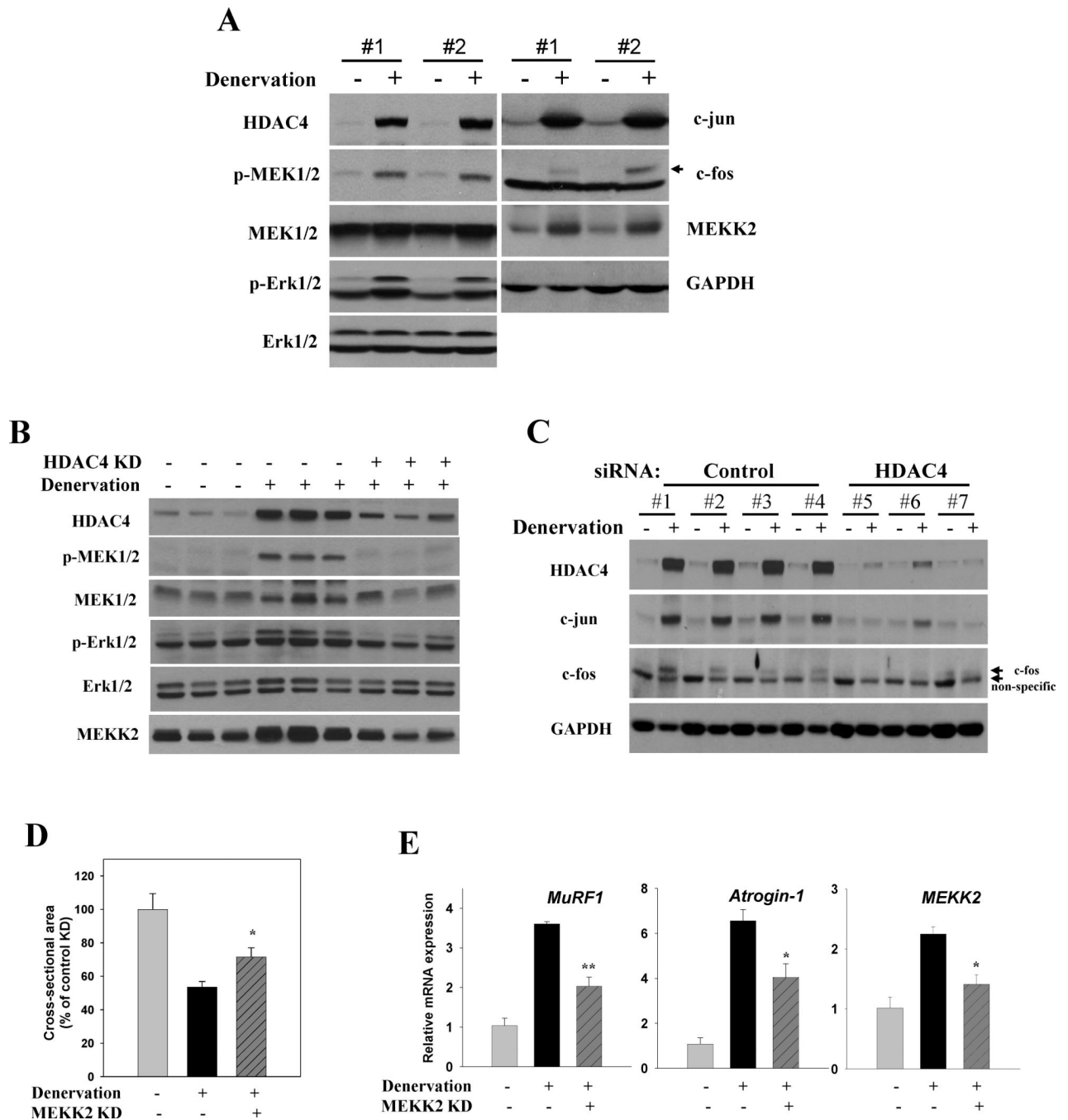
**Figure 5.**

MEKK2 is required for HDAC4 to activate AP1 and MEK1. (A) The inhibition of AP1 activity by MEKK2 KD in HDAC4-overexpressing cells. Columns, mean; Bars, SD ( $n = 3$ ). \*\* $P < 0.01$  versus HDAC4 overexpression. (B) Effect of MEKK2 KD on MEK1 activation induced by HDAC4. Activation of MEK1 was determined by immunoblotting with the phospho-MEK1/2 antibody. (C) Suppression of AP1 activity by double inhibition of MEKK2 and MEKK4 in HDAC4-overexpressing C2C12 cells. MEKK2 and MEKK4 were inhibited by transfecting dominant negative (DN) mutants in C2C12 myoblasts, and AP1 activity induced by HDAC4 was measured by luciferase assay. Columns, mean; Bars, SD ( $n = 3$ ). \*\* $P < 0.01$  versus HDAC4 overexpression.



**Figure 6.** MEKK2 is subject to reversible acetylation, and HDAC4 promotes MEKK2 deacetylation. (A) Detection of acetylated MEKK2 induced by CBP. Myc-tagged MEKK2 was co-transfected with CBP WT or catalytic-inactive mutant (CAD) into 293T cells. Immunoprecipitated MEKK2 was then subject to immunoblotting with an antibody for acetylated lysine (Ac-K). (B) HDAC4 interacts with MEKK2. 293T cells were co-transfected with Flag-HDAC4 and HA-MEKK2. Cell lysates were immunoprecipitated and immunoblotted with the indicated antibodies. (C) Deacetylation of MEKK2 by purified HDAC4 WT but not by HDAC4 CAD mutant. (D) Deacetylation of MEKK2 by HDAC4 in denervated muscle for 3 days. (E) Quantification of MEKK2 acetylation and HDAC4 expression from

independent Western blot experiments. MEKK2 acetylation and HDAC4 expression were normalized to total MEKK2 and to GAPDH expression, respectively. Columns, mean; Bars, SD ( $n = 4$ ). \* $P < 0.05$ , \*\* $P < 0.01$ , \*\*\* $P < 0.001$  (unpaired Student's  $t$ -test). (F) Reduction of acetylated MEKK2 levels in MEKK2-K385M construct mutated at Lys 385, a residue required for ATP binding and MEKK2 kinase activity. (G) The effect of MEKK2 acetylation on kinase activity. Proteins coding MEKK2 WT or K385Q were incubated with a substrate, HA-MEK1-K97M. Kinase activity was assessed by immunoblotting with p-MEK1/2 antibody.

**Figure 7.**

The MAPK signaling cascade is activated in denervated muscle and is required for proper execution of neurogenic muscle atrophy. (A) Activation of the HDAC4-MAPK-AP1 axis during denervation. Innervated and 4-day denervated muscles were immuno-blotted for MAPK components with the indicated antibodies. (B) Inhibition of MAPK signaling by HDAC4 KD in denervated muscle. Western blot analysis was performed using lysates from TA muscles electroporated with control or an HDAC4-specific siRNA followed by 5 days of denervation. (C) HDAC4-dependent AP1 induction in denervated muscles for 7 days. (D) Quantification of mean fiber CSA in TA muscle of control KD, control KD-denervated, and MEKK2 KD-denervated mice 7 days after denervation. Values are expressed as percentage



of control KD ( $n = 3$  for each group).  $*P < 0.05$  versus control KD-denervated (unpaired Student's  $t$ -test). (E) Effect of MEKK2 KD on the expressions of ubiquitin E3 ligases. Expressions of *MuRF1*, *atrogen-1*, and *MEKK2* were determined by real-time RT-PCR in TA muscles that were electroporated with control or MEKK2 siRNA and denervated for 10 days. Values were normalized to GAPDH. Columns, mean; bars, SEM.  $n = 3$  for each group.  $*P < 0.05$ ,  $**P < 0.01$  versus control siRNA DEN (unpaired Student's  $t$ -test).